https://doi.org/10.5194/egusphere-2026-5322
Preprint. Discussion started: 9 September 2026
© Author(s) 2026. CC BY 4.0 License.

A method for representing cities in global hydrological models

Naota Hanasaki[1], Kiyoharu Kajiyama[2,3], Yuga Takahashi[2,4], Kazufumi Yabu[2], Yuika Maniwa[2], Shinjiro Kanae[2]

[1]National Institute for Environmental Studies, Tsukuba 3058506, Japan
[2]Institute of Science Tokyo, Tokyo, 1528550, Japan
[3]AI-Transformed Aerospace Research Center, Korea Advanced Institute of Science and Technology, Daejeon 34141, Republic of Korea
[4]Nippon Koei Co., Ltd., Fukuoka, 812-0007, Japan

Correspondence to: Naota Hanasaki (hanasaki@nies.go.jp)

Abstract. Due to increased computational resources and the availability of fine-scale global data, global hydrological models have begun to run at spatial resolutions that resolve major cities worldwide. Because water supply in cities is achieved by a set of infrastructure, traditional grid-level or basin-level modeling and assessment do not provide reliable and interpretable results for cities. Here, we propose a generic city sub-model for global hydrological models to express the water supply in cities. Using a newly developed global gridded database of city areal extent, we conducted a series of global hydrological simulations focusing on municipal water supply for 11 representative cities. Although the model was uncalibrated and forced with global data, the simulation performed reasonably for these cities. The results improved further when additional data on external water sources were taken into account. The subsequent city-level water assessment provides a single water scarcity score for each city. It is more interpretable than the traditional grid- or basin-level assessment, which typically shows a wide range of scores across grid cells or basins or includes non-urban regions. This study highlights the importance of representing cities in global hydrological models and water scarcity assessments, and the need to develop a comprehensive global database of urban water supply. This study opens a pathway toward city-level global water assessments using generic global hydrological models.

1 Introduction

Although water is a renewable and abundant resource of the Earth, water scarcity is reported in many places in the world (Vörösmarty et al., 2000). Water scarcity is exacerbated by climate change and socio-economic development, which destabilize water availability and increase water requirements, respectively (Alcamo et al., 2003;Schewe et al., 2014). Additionally, more people live in cities than in towns or rural areas (United Nations, 2025). It underscores the urgent need for city-level global water scarcity assessments, as both the cause (i.e., water requirement) and the effect (i.e., population and economic activity under risk of water scarcity) are increasing. In this study, water scarcity refers to an insufficient supply of water to meet water requirements.

https://doi.org/10.5194/egusphere-2026-5322
Preprint. Discussion started: 9 September 2026
© Author(s) 2026. CC BY 4.0 License.

To quantitatively assess water scarcity worldwide, global hydrological models (GHMs) with explicit representation of water use and management have been developed (Müller Schmied et al., 2024;Sutanudjaja et al., 2018;Hanasaki et al., 2018a;Burek et al., 2020). These models were calculated at a spatial resolution of 30 arc minutes (approximately 55 km at the Equator), while some recent GHMs have been simulated at substantially higher spatial resolutions. Wada et al. (2016) conducted the first global 6-arc-minute simulation using the PCR-GLOBWB model and presented a grid-level assessment of water scarcity. They identified water scarcity in grid cells containing large cities (e.g., New York), but one cannot take their results at face value, as water availability and requirements do not necessarily balance for each grid cell in reality. Flörke et al. (2018) conducted the first global city-level water scarcity assessment for 482 cities. They used the city-specific water source database (typically, dams and weirs) compiled in McDonald et al. (2014) and estimated water availability at each water source by using the WaterGAP model's 5-arc-minute simulations. They identified cities at high risk of water scarcity, although the applicability is constrained by the coverage of the database. He et al. (2021) and Vanham et al. (2021) adopted a similar approach to Wada et al. (2016), and counted the number of the urban population under water stress using the HYDE global gridded database (Klein Goldewijk et al., 2017). These studies have initiated city-level global water scarcity assessments, but because the spatial extent of large cities is extensive (i.e., under the spatial resolution of 5-6 arc minutes, a city is no longer within a single grid cell), and water supply and demand do not necessarily close within each cell, further improvement in GHMs is essential to represent cities in the world.

In this study, we propose a new method for representing cities in GHMs. We work on a spatial resolution of 5 arc-minutes for GHMs, given current input data availability. As the literature survey revealed, there are three key challenges. First, since cities span multiple grid cells, it is necessary to cluster these grid cells and treat them as hydrologically connected units. Second, as cities are numerous and expanding, while data access is often limited, it is necessary to keep the sub-model flexible and simple. Third, because cities do not withdraw water solely from their upstream watersheds, it is necessary to allow for water sources to be located in remote areas (hereafter external water sources). We pose two research questions. How well can we represent the hydrological process of “cities” in GHMs? What is the advantage of city-level water scarcity assessment compared to the traditional basin-level or grid-level assessments? We use the global hydrological model H08 (Hanasaki et al., 2018a) to discuss whether the new sub-model enables a global city-level water scarcity assessment. To narrow the scope of the model development, we will not modify existing sub-models or parameters.

2 Methods

2.1 Model

2.1.1 The H08 global hydrological model

H08 is a GHM that includes water use and management processes (Hanasaki et al., 2008a;Hanasaki et al., 2018a). It is a gridded model that subdivides land into equal-sized grid cells (the standard spatial resolution is 30 arc minutes, or about 55

https://doi.org/10.5194/egusphere-2026-5322
Preprint. Discussion started: 9 September 2026
© Author(s) 2026. CC BY 4.0 License.

km at the equator). It consists of six sub-models: land surface hydrology, river routing, crop growth (for irrigation water estimation), reservoir operation, non-irrigation water use (industrial and municipal water), and environmental flow (Hanasaki et al., 2018a). These sub-models calculate the hydrological state variables and fluxes under physical and empirical laws. The land surface hydrology sub-model has two soil layers representing unsaturated and saturated zones and solves surface water and energy balances. The crop growth sub-model calculates daily crop development, but in H08, it is primarily used to estimate irrigation timing and duration worldwide. The reservoir operation sub-model controls the release and storage of individual reservoirs using the algorithm described in Hanasaki et al. (2006). The non-irrigation water use sub-model abstracts water from various sources. The function is described in detail in the next paragraph. The environmental flow sub-model determines the minimum discharge rate to be maintained in river sections by using a globally uniform algorithm. This sub-model is disabled in this study because it is unclear how environmental flow rates are set and whether they are being adhered to at the individual-city scale. The temporal resolution is 1 day, and the sub-models exchange variables at this interval. The model is designed to close the water balance at each grid cell and time step. In this study, we develop a new sub-model to represent urban water processes.

H08 considers three water-use sectors (agricultural, industrial, and municipal), and seven water sources. There are five surface water sources: river (including reservoirs' operation that regulate flows), storage in local reservoirs (not regulating river flows and acting as water tanks; note that due to high spatial resolution of this study no local reservoir is considered in this study), aqueducts (water transfer from surrounding grid cells), seawater desalination (Hanasaki et al., 2016;Ai et al., 2022), and unspecified surface water (USW). USW is a hypothetical surface-water component to close the gap between surface-water requirement and availability. There are two groundwater sources: renewable groundwater (water in the saturated soil layer) and non-renewable groundwater (NRGW; abstraction from a hypothetical deep layer assumed non-renewable and available only after depletion of the saturated soil layer). Water is balanced at each grid cell and time step (a day) for both natural and human aspects. That is, precipitation is partitioned between evapotranspiration and runoff, and water requirements are first partitioned into surface water and groundwater, then into five and two sources, respectively. H08 can take three options regarding human water balance. One is to meet supply and demand, ensuring that daily water demand is always met by water sources, including NRGW and USW. The others are to restrict the water supply based on the availability of six water sources (excluding USW) or five (excluding both USW and NRGW). In this study, the first option was taken. See discussion in Hanasaki et al. (2018a) for advantages and disadvantages of each.

2.1.2 City sub-model

The concept of the city sub-model is shown in Fig. 1. Assuming a river flows through a city consisting of multiple grid cells (Fig. 1a), and water use is distributed as shown in Fig. 1b. When a traditional grid-level water scarcity assessment is conducted using the water stress index (water withdrawal relative to water availability), water stress is distributed as shown in Fig. 1c: water is abundant in cells containing the main streams, while scarce in those without. Also, GHMs assume that return flow (the unconsumed/unevaporated portion of water withdrawal) is released into the adjacent downstream grid cell. This results in

https://doi.org/10.5194/egusphere-2026-5322
Preprint. Discussion started: 9 September 2026
© Author(s) 2026. CC BY 4.0 License.

cyclic water use within a city, which is unrealistic. Here, we assume that water demand within a city is aggregated at the inlets (Fig. 1d). The inlets are the grid cells within the city boundary where major rivers flow in. It is assumed that the grid cell likely contains water treatment plants and the head of the water pipeline that supplies water within the city boundary. Return flow is aggregated and released at the outlets (Fig. 1d). The outlets are the grid cells where major rivers flow out. It is assumed that the grid cell likely contains wastewater treatment plants and the terminal of the sewage pipeline that collects wastewater within the city boundary. The water scarcity index is calculated for the aggregated value across the city; it is uniform within the city boundary (Fig. 1e).

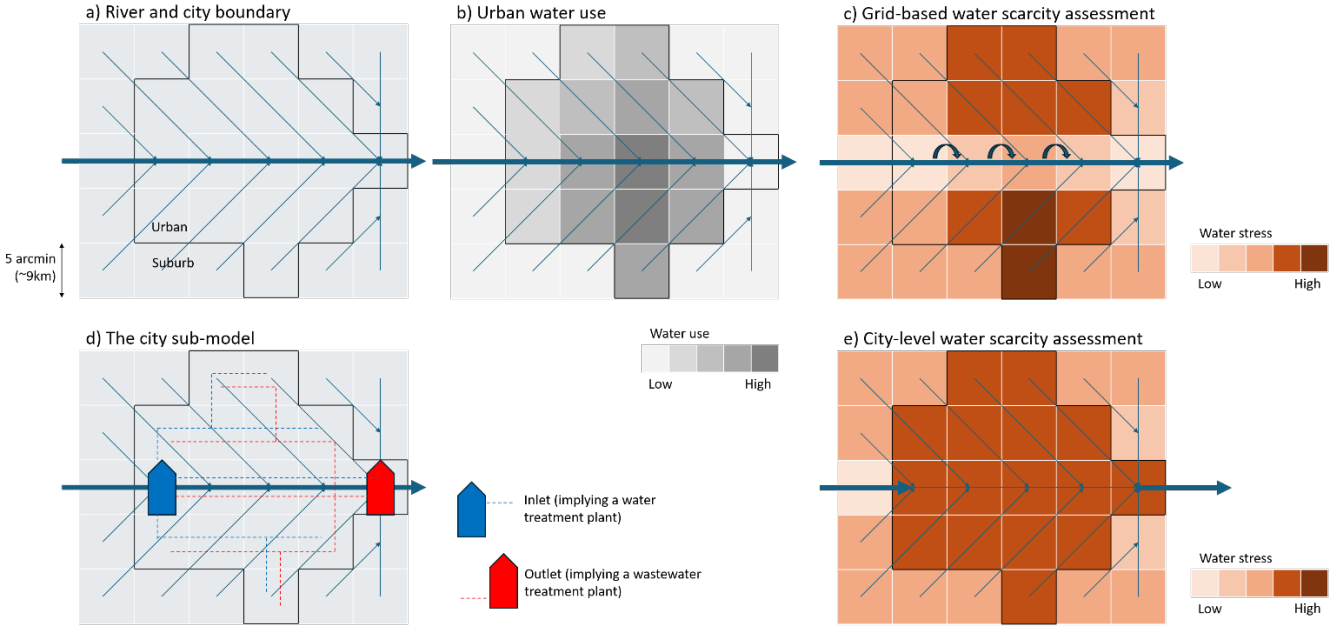

Figure 1. Schematic diagram of the city sub-model for a hypothetical map. a) River and city boundary. The solid black and blue lines are the city boundary and the river channels, respectively. Thick arrows indicate the main channel, which is rich in water availability. b) Urban water use. The dark color indicates the concentration of urban water use. c) Grid-based water scarcity assessment. d) Conceptual diagram of the city sub-model. The blue and the red symbols indicate the inlet and outlet, respectively. e) City-level water scarcity assessment.

2.2 Data

2.2.1 Boundary conditions for H08

[Meteorological data] To run H08, we need eight daily meteorological variables, namely, air temperature, specific humidity, wind speed, relative humidity, downward shortwave radiation, downward longwave radiation, rainfall, and snowfall. We used the W5E5 (Lange et al., 2021) global meteorological dataset at the spatial resolution of 30 arc minutes. W5E5 is a merged dataset of the WATCH Forcing Data methodology applied to ERA5 reanalysis, called WFDE5 (Cucchi et al., 2020) over land with ERA5 data over the ocean. First, we linearly interpolated W5E5 into 5 arc minutes. Then we applied elevation adjustments to air temperature and surface air pressure using the MERIT DEM global elevation dataset at 5-arc-minute resolution

https://doi.org/10.5194/egusphere-2026-5322
Preprint. Discussion started: 9 September 2026
© Author(s) 2026. CC BY 4.0 License.

(originally 3-arc-second) (Yamazaki et al., 2017). Finally, we applied rainfall-snowfall separation at a 5-arc-minute resolution. The methods of elevation correction and rainfall-snowfall separation are shown in Appendix A. We prepared the data from 2010 to 2019.

To run H08, we need numerous input data (boundary conditions). We used the standard H08 input data as shown in Table 1 of Hanasaki et al. (2018a). Among 16 variables listed in the table, three variables, namely albedo, soil texture, and permafrost and glacier, were originally distributed at a 60- and 30-arc-minute spatial resolution, respectively, and interpolated to 5 arc minutes. Four variables, namely relief, hydrogeology, irrigated area, and crop species, were originally distributed at a 5-arc-minute spatial resolution and were therefore used directly. For the flow direction map, we replaced DDM30 (Döll and Lehner, 2002) at 30-arc-minute resolution with MERIT Hydro (Yamazaki et al., 2019) at 5-arc-minute resolution. The aqueduct network was generated at 5 arc minutes, using the algorithm of Hanasaki et al. (2018a). These aqueducts are called implicit aqueducts and represent short-distance, gravity-driven water transfer between grid cells. Another type, called explicit aqueducts, is discussed later. Reservoirs in the global inventory of Lehner et al. (2011) were manually geo-referenced to the flow direction map. Crop intensity, irrigation efficiency, groundwater fraction of water use, municipal water withdrawal, industrial water withdrawal, and gross domestic product (GDP) are country/region specific, hence distributed using the national boundary data of Gridded Population of the World version 4 (GPW4) (Center for International Earth Science Information Network-CIESIN-Columbia University, 2017). For the former three variables, we assumed the national value was uniformly distributed. For the latter three variables, we weighted by the GPW4 population distribution. Table 1 summarizes all input data.

Table 1. Selected input data used in this study.

	Name	Original resolution	Interpolation	Reference
Meteorological data	W5E5	30 arc minutes	Linear	Lange et al. (2021)
Elevation	MERIT DEM	5 arc minutes	-	Yamazaki et al. (2017)
River network	MERIT Hydro	5 arc minutes	-	Yamazaki et al. (2019)
City boundary	HydroUrbanMap (HUM)	5 arc minutes	-	Kajiyama et al. (2026)
Other land conditions	H08 standard inputs	5 - 60 arc minutes or country-wise	Linear	Hanasaki et al. (2018a)

2.2.2 City boundary data

For city boundary data, we used the HydroUrbanMap (HUM) (Kajiyama et al., 2026). HUM is a global gridded dataset at the spatial resolution of 5 arc minutes. It contains city boundaries, inlets, and outlets. The global city boundary contains 1604 cities listed in the World Urbanization Prospects (United Nations, 2019). The spatial extent of each city was estimated using the GPWv4 global gridded population data (Center for International Earth Science Information Network-CIESIN-Columbia University, 2017), and grid cells were clustered by summing their populations until the total matched the reported city

https://doi.org/10.5194/egusphere-2026-5322
Preprint. Discussion started: 9 September 2026
© Author(s) 2026. CC BY 4.0 License.

population. The inlet and outlet grid cells of a city are defined as the uppermost and lowermost grid cells within its boundary. HUM and this study are fully consistent, as both use the MERIT Hydro flow direction map (Yamazaki et al., 2019).

2.3 Expression of cities and rivers

We adopted the regional classification by Kummu et al. (2010) as shown in Table 2. Because it divides the world into 12 regions, we call it K12. Then we listed the largest cities in each region (12 in total). The United Nations geoscheme, which divides the world into 22 regions (UN22), is more widely used, as shown in Table 2. Here, we excluded or replaced five cities for this study. First, Cairo on the Nile River was excluded from this study from a simulation viewpoint. The Nile River is the fourth-largest river basin in the world. The source areas are in the upstream, where meteorological monitoring is sparse (e.g., Su et al. (2026)). Moreover, the hydrological elements, including lakes, swamps, deserts, reservoirs, and irrigation, make the large-scale river discharge simulation challenging (e.g., Di Vittorio and Georgakakos (2021)). Consequently, this basin has been poorly represented in GHMs and has often been excluded from global model intercomparisons (Haddeland et al., 2011;Zaherpour et al., 2018). Next, three cities were replaced with others from a water-scarcity assessment perspective. Replacement has been carried out among the world's 100 largest cities within the same region. Lagos was replaced by Cape Town, which experienced severe water scarcity in the 2010s, peaking between 2017 and 2018 (LaVanchy et al., 2019). Similarly, New York was replaced by Los Angeles, and Delhi by Chennai. Lastly, Manila was replaced with Bangkok because more public data was available.

Table 2. Eleven studied cities. K12 region corresponds to the 12 world regions proposed by Kummu et al. (2010). UN22 region shows the corresponding regions in the United Nations geoscheme. The largest cities are the most populous in each K12 region. Studied cities show that some were replaced by other top 100 cities in the same K12 region.

K12 region	UN22 region	Largest cities	Studied cities
North Africa	Northern Africa	Cairo	--
Middle and South Africa	Eastern, Middle, Southern, and Western Africa	Lagos	Cape Town
North America	Northern America	New York	Los Angeles
Central America	Caribbean and Central America	Mexico City	Mexico City
Latin America	South America	São Paulo	São Paulo
Eastern Asia	Eastern Asia	Tokyo	Tokyo
Southeastern Asia	Southeastern Asia	Manila	Bangkok
South Asia	South Asia	Delhi	Chennai
Middle East	Middle East	Istanbul	Istanbul
Eastern Europe and Central Asia	Central Asia and Eastern Europe	Moscow	Moscow
Western Europe	Northern, Southern, Western Europe	Paris	Paris

https://doi.org/10.5194/egusphere-2026-5322
Preprint. Discussion started: 9 September 2026
© Author(s) 2026. CC BY 4.0 License.

Australia and Oceania	Australia and New Zealand, Melanesia, Micronesia, and Polynesia	Sydney	Sydney

Figure 2 shows the study domains of 11 cities. Four cities have one set of inlet and outlet grid cells (see also Table 3). Among them, the main stem of a major river runs through 2 cities: Bangkok (the Chao Phraya River; Fig. 2g) and Paris (The Seine River; Fig. 2b). For these cases, the study domain is configured as the entire basin. For the remaining two cities, we do the same for a major tributary or the upper basin of an important confluence: São Paulo (the Tietê River, a major tributary of the La Prata River; Fig. 2j) and Moscow (the Volga River above the confluence of the Oka River; Fig. 2c). The remaining seven cities have multiple rivers flowing in and out of the city boundary; hence, there are more than two sets of inlet and outlet grid cells. In two cities, municipal water is supplied from rivers flowing into: Tokyo (the Tone, the Ara, the Tama, and the Sagami Rivers), and Sydney (the Nepean, the Woronora, and the Parramatta Rivers). In five cities (Cape Town, Los Angeles, Mexico City, Chennai, and Istanbul), municipal water supplies rely substantially on external water sources that do not flow into the cities; details are discussed in the next paragraph.

In reality, many cities rely on external water resources. We conducted an intensive survey of the water sources of the studied cities and identified major external sources (see Table 3). Cape Town receives water from the Sonderend River, a neighboring basin in the west. Mexico City uses water resources from the Lerma River in the west and the Cutzamala River in the southwest. São Paulo receives water from the Paraíba do Sul River in the west. Istanbul receives water from the Melen River, located approximately 200 km to the east. The study domains for these cities include the basins mentioned (Figures 2d, e, f, k). The case of Moscow is a bit complex. The Moscow River flows through the city of Moscow, which is a tributary of the Oka River, a major tributary of the Volga River. Moscow receives water from the Moscow River and the Volga River (flowing north). This is why the study domain of Moscow includes the Volga River above the confluence of the Oka River (Fig. 2c). Los Angeles receives water from the Owens River system (300 km to the north) through the Los Angeles Aqueduct, the Sacramento-San Joaquin River system (500 km to the northwest) through the California Aqueduct, and the Colorado River (400 km to the west) through the Colorado River Aqueduct. Chennai receives water from the Krishna River (400 km to the north). Because the source rivers are distant and their catchment areas are extensive for these two cities, we do not extend the domain and apply water at a fixed rate (Table 3).

To incorporate the external water sources, we utilize the existing H08 function, termed the explicit aqueducts. In contrast to the implicit aqueduct, it enables water transfer between any two points (the origin and the destination) irrelevant to elevation. One condition is that, due to the formulation of the H08 model, the river sequence (i.e., the order of cells from upstream to downstream) of the origin must be greater than that of the destination. In this study, we confirmed the external water sources for five cities (Table 3) and configured them as the origins of explicit aqueducts. We set the corresponding city water inlets as the destinations. When water in a destination grid cell is depleted, water is transferred from an origin grid cell to the destination cell, with water-balance closure.

https://doi.org/10.5194/egusphere-2026-5322
Preprint. Discussion started: 9 September 2026
© Author(s) 2026. CC BY 4.0 License.

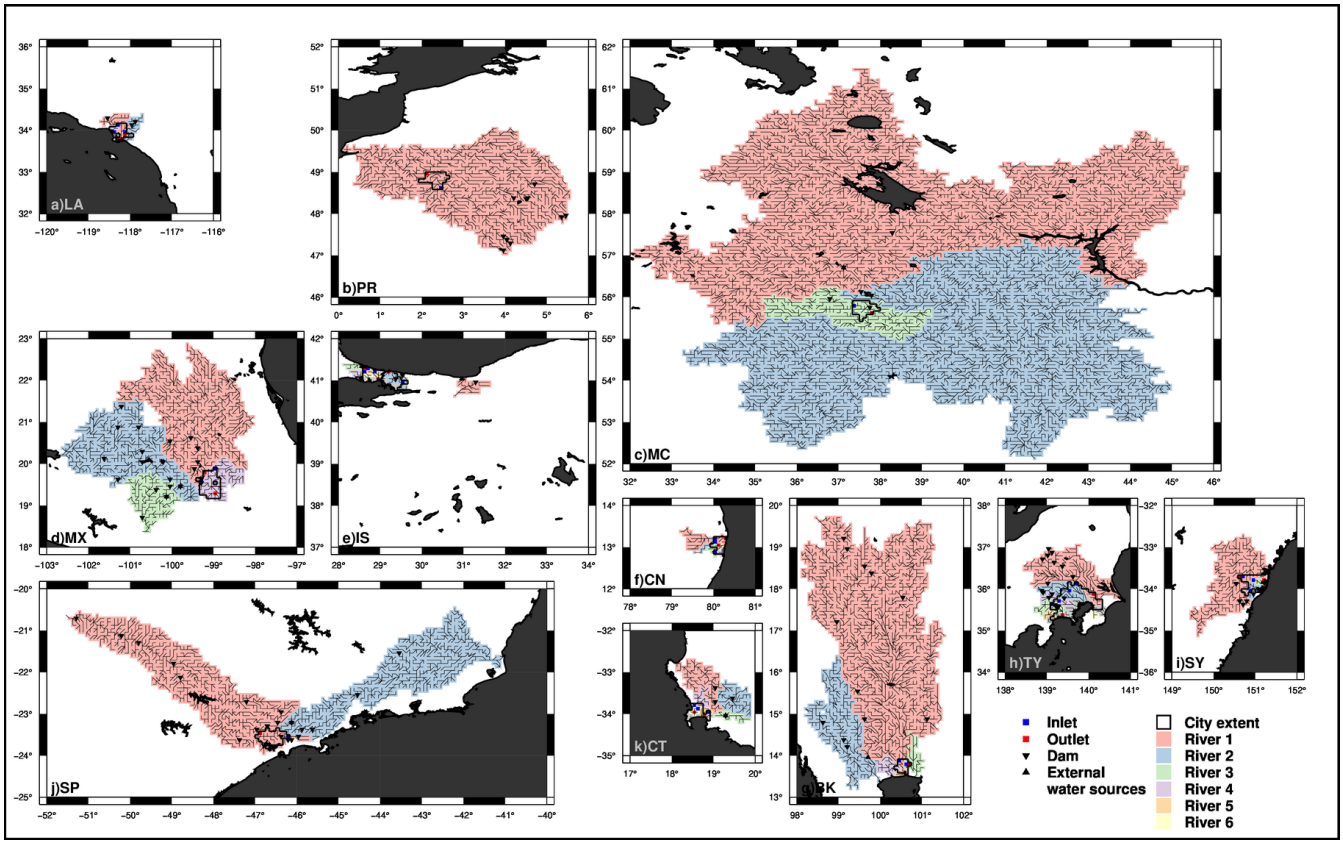

Figure 2. Study domain of cities. a) Los Angeles (LA), b) Paris (PR), c) Moscow (MC), d) Mexico City (MX), e) Istanbul (IS), f) Chennai (CN), g) Bangkok (BK), h) Tokyo (TY), i) Sydney (SY), j) São Paulo (SP), and k) Cape Town (CT). River 1 – 6 denote the largest to the sixth largest river basins in each study domain. The names of the rivers are shown in Table 3.

Table 3. Cities and their water sources. R for river and A for aqueduct. Numbers in brackets are the river ID in Fig. 2.

City	Rivers flow in	External sources	Discharge validated	Source of water use data
Cape Town	Diep R [4] Eerste R [5] Salt R [6]	Sonderend R [3] (Theewaterskloof Dam)	Malmesbury, Diep R [4]	GreenCape (2019)
Los Angeles	Los Angeles R [1] San Gabriel R [2] Ballona Creek [3]	California A Colorado River A Los Angeles A (80 $m^3 s^{-1}$)	Whittier Narrows Dam, San Gabriel R [2]	Los Angeles Department of Water and Power (LADWP) (2023)

https://doi.org/10.5194/egusphere-2026-5322
Preprint. Discussion started: 9 September 2026
© Author(s) 2026. CC BY 4.0 License.

Mexico City	Moctezuma R [1] Lake Texcoco [4]	Lerma R [2] (José Antonio Alzate Dam) Cutzamala R [3] (Valle de Bravo dam)	Salamanca, Lerma R [2]	Medina-Rivas et al. (2022)
São Paulo	Tiete R [1]	Paraíba do Sul R [2] (Jaguari Dam)	Branca, Paraíba do Sul R [2]	Secretaria Nacional de Saneamento (SNS) Ministério do Desenvolvimento Regional (MDR) (2020)
Tokyo	Tone R [1] Ara R [2] Sagami R [3] Tama R [4]	--	Yattajima, Tone R [1]	Water Resources Department Water Management and Land Conservation Bureau Ministry of Land Infrastructure Transport and Tourism (MLIT) (2025)
Bangkok	Chao Phraya R [1]	Mae Klong [2] (Mae Klong Dam)	Nakhon Sawan, Chao Phraya R [1]	Metropolitan Waterworks Authority (2024)
Chennai	Kosasthalaiyar R [1] Cooum R [2] Adyar R [3]	Krishna R and desalination plants (5 $m^3 s^{-1}$)		The Energy and Resources Institute (TERI) (2021)
Istanbul	Riva R [2] Kumluca R [3] Kagithane R [5] Sazlidere R [6]	Melen R [1] (Melen Dam)	Botbasi, Sakarya R	Turkish Statistical Institute (2023)

https://doi.org/10.5194/egusphere-2026-5322
Preprint. Discussion started: 9 September 2026
© Author(s) 2026. CC BY 4.0 License.

Moscow	Moscow R [3] (a tributary of the Oka R [2])	Volga R [1] (Ivankovo Dam)	Stritsa, Volga R [1]	Interfax-Russia (2022)
Paris	Seine R [1]	--	Paris, Seine R [1]	OECD (2025)
Sydney	Nepean R [1] Woronora R [2] Parramatta R [3]	--	Penrith, Nepean R [1]	Sydney Water (2024)

2.4 Simulation

In this study, we set up H08 in three ways. The first is the original model, or without the city sub-model. Hereafter, we call this the control simulation (CTR). This configuration is similar among GHMs, including the earlier study of Wada et al. (2016) and others. The second is the model with the city sub-model (URB). Other settings are identical to CTR. The third is the same as URB, but it adds external water sources (i.e., other than river discharge at inlets; EXT). These sources are identified through an intensive internet survey shown below. CTR and URB are readily applicable globally, whereas EXT is not. For all simulations, the period is from 2010 to 2019, with a daily interval. To save computer resources, the simulations were conducted for each city. This was done by setting simulation domains for each city, including the relevant basins as discussed below. The simulation domain was configured to cover the entire watershed whenever possible; however, when the watershed was very large, it covered only the major tributaries (see Section 3.1.1).

2.5 Validation and assessment

First, to validate the estimated water availability of cities, the river discharge at the upstream point was used (Table 3). First, we collected monthly river discharge data of the rivers flowing to the cities at the Global Runoff Data Centre (GRDC). In case those rivers are not found in GRDC, namely Istanbul, we collected data on rivers flowing outside the boundary, namely the Sakarya River. Because of data limitations, the long-term monthly mean value was compared. We adopt the KGE score as river discharge evaluation score as defined below

$$KGE = 1 - \sqrt{(1-r)^2 + (\alpha - 1)^2 + (\beta - 1)^2} \quad (1)$$

where r is the Pearson correlation coefficient, $\alpha = \sigma_s/\sigma_o$ (the ratio of simulated to observed standard deviation), and $\beta = \mu_s/\mu_o$ (the ratio of simulated to observed mean). KGE takes -0.41 when the river discharge is identical to the observed annual mean, which is considered a threshold for a model to have predictability (Knoben et al., 2019). Next, we collected annual per capita water withdrawal for selected cities from various sources, shown in Table 3. The validation of the city boundary, inlets, and outlets is provided in Kajiyama et al. (2026).

https://doi.org/10.5194/egusphere-2026-5322
Preprint. Discussion started: 9 September 2026
© Author(s) 2026. CC BY 4.0 License.

To assess water scarcity, the Cumulative Abstraction to Demand (CAD) index was used (Hanasaki et al., 2008b;Hanasaki et al., 2018b).

$$CAD = \frac{\sum_d a_d}{\sum_d d_d} \quad (2)$$

Where a_d and d_d denote water available and demand for day d. The symbol Σ denotes summation over the study period. Note that $a_d \leq d_d$, which means daily water abstraction equals the day's water demand when water is abundant, and is below that when water availability is constrained. The CAD index expresses whether water demand is met over the study period. The values 0 and 1 in the index represent cases where demand was not met at all and always fully met, respectively. Hanasaki et al. (2018b) argued that CAD scores >0.99, >0.8, and >0.5 are categorized as low, moderate, and high stress, respectively. The index accounts for the seasonality of water availability and demand: water abundance in the wet season is not carried over into the dry season unless upstream reservoirs regulate the flow. Although the original CAD accounts for agricultural, industrial, and municipal water demands, this study excludes agricultural water demand within the city boundaries because we focus on the 11 most populous cities in the world, where agricultural water is essentially negligible. The simulation for out-of-city areas includes the agricultural water abstraction.

3 Results and Discussion

3.1 Validation

3.1.1 Discharge

The goal of this model development is to propose a novel geographical unit of water scarcity assessment. Since the assessment metric CAD focuses on the balance between water availability and withdrawal, we examined the simulation results for these two elements in the cities studied. Note that enhancing their accuracy is beyond the scope of this paper: as discussed in detail below, it largely relies on the quality and quantity of input and validation data. The discussion below is to be used to interpret the assessment below (Section 3.2).

Figure 3 shows the mean monthly river discharge of 10 cities for the URB runs. As discussed in Section 2.4, observed river discharge near Chennai was not found. The KGE score exceeded -0.41 in six cities (Los Angeles, Tokyo, Istanbul, Moscow, Paris, and Sydney). In Istanbul and Moscow, all three KGE factors (r, α, and β) take reasonably good scores, resulting in relatively high KGE scores. In Los Angeles, Tokyo, Paris, and Sydney, one of the factors is inferior, namely, r (correlation coefficient, or runoff seasonality), r, α (variation, or the amplitude of runoff variation), and α, respectively. These are attributed to over-regulation by reservoirs between April and December, earlier peak arrival, and over- and underestimation of peak flows, respectively. The KGE score falls far below -0.41 in four cities (Cape Town, Mexico City, São Paulo, and Bangkok), which is obviously attributed to substantial overestimation of river flows except for São Paulo.

As seen in earlier literature, the site-specific river discharge metrics in global hydrological simulation are not as high as well-calibrated basin-scale studies (Zaherpour et al., 2018;Heinicke et al., 2024). We state our views on this. First, the parameters

https://doi.org/10.5194/egusphere-2026-5322
Preprint. Discussion started: 9 September 2026
© Author(s) 2026. CC BY 4.0 License.

of global hydrological models are not fine-tuned for each basin. If tuned, the issues seen in Los Angeles, Tokyo, Paris, and Sydney (i.e., one of the three KGE factors is problematic) may be relatively easy to address. Parameter tuning of GHMs has been studied for decades, but it remains challenging largely due to a lack of reliable input and validation data (Yoshida et al., 2022). Second, the issue observed in Cape Town and Mexico City is difficult to address: hydrological simulation in arid and intensively managed basins is always challenging (Wheater, 2025). Because we may substantially overestimate the water resources in these cities, we should pay attention to the assessment results. Third, the issue observed in Bangkok is a fundamental water-energy balance (i.e., input data) problem. Although the basin is intensively developed, the catchment area exceeds 160,000 km^2 and receives more rainfall than the global average. Our simulation results indicate a considerable underestimation in evaporation, which implies there are problems with radiation data, since precipitation is reasonable in this basin. Although one notices such a problem, site-specific modification of global meteorological data is challenging, if not impossible. Lastly, the relatively low KGE score in São Paulo should not be taken seriously, as there is little seasonal variation in both observation and simulation, and the mean discharge is reasonably well simulated ($\beta = 1.34$).

https://doi.org/10.5194/egusphere-2026-5322
Preprint. Discussion started: 9 September 2026
© Author(s) 2026. CC BY 4.0 License.

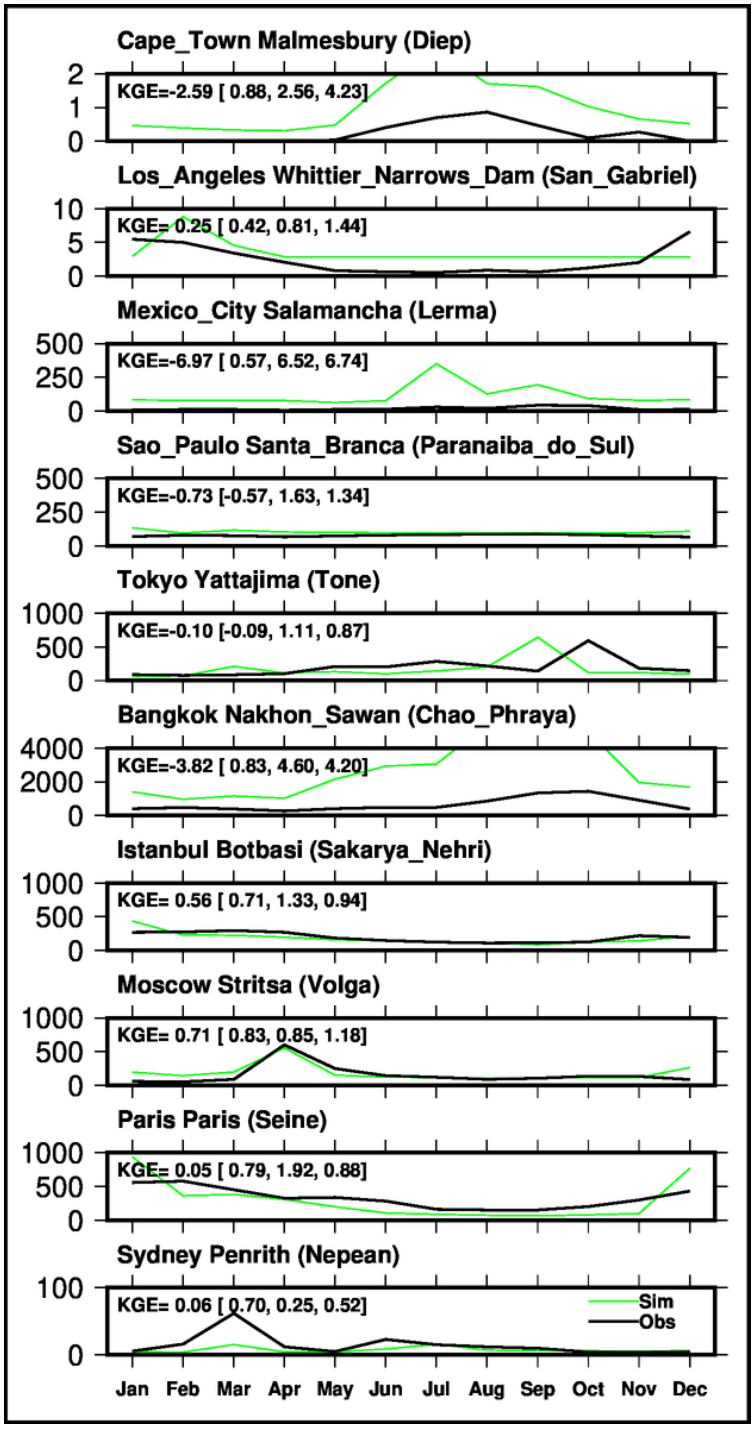

Figure 3. Mean monthly discharge for 10 cities. River discharge for the rivers relevant to Chennai was not available. Black and green lines show observed and simulated river discharge, respectively. Numbers in brackets show the three factors composing KGE, namely, the correlation coefficient (r), the α (the ratio of simulated to observed standard deviation σ), and the β (the ratio of simulated to observed mean μ). The unity indicates the perfect value for each factor.

https://doi.org/10.5194/egusphere-2026-5322
Preprint. Discussion started: 9 September 2026
© Author(s) 2026. CC BY 4.0 License.

3.1.2 Water withdrawal

Next, we compared the amount of water withdrawal used in the simulation and the reported value by local authorities. As briefly mentioned in the methods section, because reliable global gridded water-use data are unavailable, we interpolated national-level municipal and industrial water data of the AQUASTAT database of the Food and Agriculture Organization (https://www.fao.org/aquastat/) with population density weights. A similar approach, which assumes homogeneity in per capita municipal water withdrawal within a country, is commonly used in GHMs (e.g., Müller Schmied et al. (2024)). Understanding the potential gap between simulated and reported water withdrawal values is critical to interpreting the assessment results. Figure 4 shows the per-person daily municipal water withdrawal for 11 cities. The errors are below 25% in seven cities (Cape Town, Los Angeles, Mexico City, São Paulo, Tokyo, Chennai, and Istanbul). Per capita water withdrawal is overestimated in Moscow, Paris, and Sydney by more than 50%, while it is underestimated in Bangkok by nearly 40%.

The gridded data preparation method assumes that per-capita municipal water withdrawal is uniform across the country; hence, the accuracy of this assumption and the national data are essential. Take a closer look at Bangkok, where one of the largest discrepancies was found. According to AQUASTAT, the national total municipal water in 2010 was 2.74 km^3 $year^{-1}$ and the total national population was 69×10^6. This yields 109 L $person^{-1}$ day^{-1}. This is the H08 model referred to. On the contrary, according to the Metropolitan Waterworks Authority (2024), which supplies municipal water for Bangkok and surrounding cities, the total water supplied is 1.52×10^9 L day^{-1}, and the population with access to their water supply is 8.15×10^6, which yields 187 L $person^{-1}$ day^{-1}. These data indicate that the homogeneity assumption may not be valid in this country. Since it is difficult to accurately and comprehensively collect data on water usage by city worldwide, the method we have adopted is considered realistic. However, when data becomes available, cross-checks such as those performed here should be conducted to verify the accuracy of the input data.

https://doi.org/10.5194/egusphere-2026-5322
Preprint. Discussion started: 9 September 2026
© Author(s) 2026. CC BY 4.0 License.

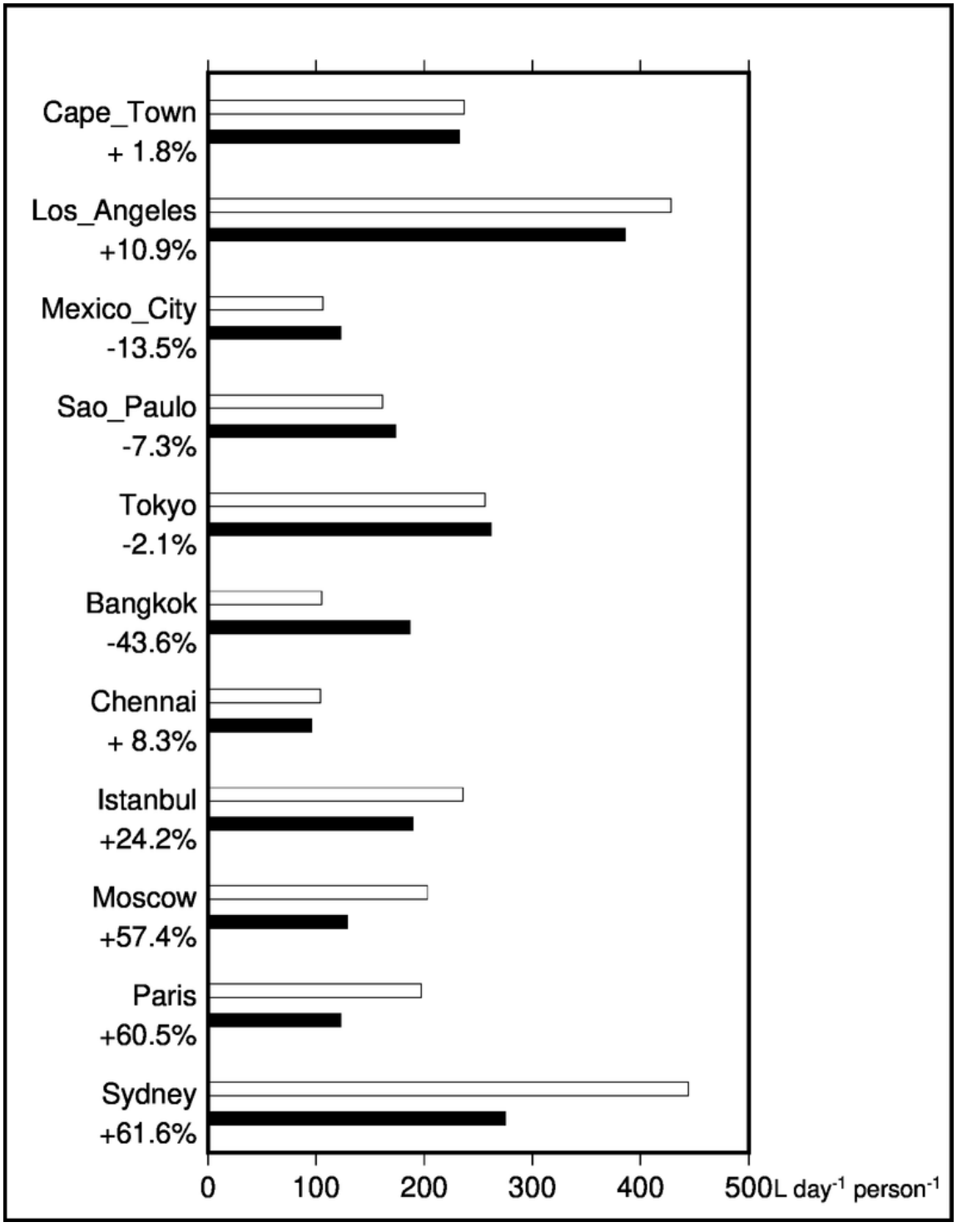

285

Figure 4. Per-person daily water withdrawal for 11 cities. The open bar is for simulation, and the filled bar is for observation. The number below the city indicates the simulation's bias (positive for overestimation, negative for underestimation).

https://doi.org/10.5194/egusphere-2026-5322
Preprint. Discussion started: 9 September 2026
© Author(s) 2026. CC BY 4.0 License.

3.2 Water scarcity assessment

[Results] Figure 5 shows the distribution of the CAD index for 11 cities. For comparison, the grid-level, city-level, and basin-level results are shown. City-level shows the results of the URB run, or employing the H08 model with the new city sub-model to represent cities without external water sources. The others show those of the CTR run, or a typical configuration of GHMs. The results including the external water sources are discussed in Section 3.3.

The grid-level results show significant variations in the CAD score within the city boundary. This is, as mentioned earlier, due to heterogeneity in water availability – water availability is high for grid cells with a main channel or a major tributary, whereas the opposite holds for those with minor stems (Fig. 1c). Because the world's largest cities are equipped with piped water supply networks, obviously, grid-based water availability has nothing to do with the actual water availability.

Next, the basin-level results show distinct patterns – the patchwork-like distribution of the CAD index. For cities with multiple river basins (e.g., Cape Town, Los Angeles, Mexico City, Tokyo, Chennai, Istanbul, and Sydney), it is hard to assess a city's water scarcity because the basins have varying levels of water scarcity. For cities located in the mid- to upstream reaches of a single large river basin (e.g., São Paulo, Moscow, and Paris), the city's water scarcity is underestimated because water use is concentrated within the city boundary, which is only a small portion of the entire basin (see Fig. 2). As shown in Table 4, the basin-level CAD exceeds the city-level CAD (e.g., in Moscow, the basin-level is 0.66 while the city-level is 0.51). Furthermore, the basin's CAD index is not comparable with others, because it depends on the catchment area and water use for purposes other than the city.

Finally, the city-level results show a single water-scarcity score for each city, reflecting the balance between the city's total water abstraction and demand at the water-inlet grid cells. It also excludes the effect of cyclic water use seen in the grid-level assessment within the city boundary (i.e., water drained in the upstream grid cell is abstracted in the next downstream grid cell) because all the drained water is transferred to the outlet grid cells.

Table 4 shows the range of the CAD index for each assessment level. As expected from Fig. 5, the range of scores for the grid-level assessment is substantial. For instance, in Tokyo, the city-level assessment score is 0.88 (low water scarcity) while the lowest and mean grid-level scores are 0.08 and 0.69. The basin-level assessment also shows substantial variation in CAD scores among rivers, ranging from 0.69 for the Tama River to 0.95 for the Sagami River. The basin-wise assessment is misleading in Tokyo because the water supply from the Tone River (CAD=0.88), which flows in the distance, plays a predominant role and compensates relatively low scores for two rivers (the Ara and the Tama Rivers), which flow through the heart of the city.

Finally, the influence of over- and underestimation in river discharge and municipal water withdrawal is discussed. Bangkok's city-based score (CAD=1.00)—where simulated river discharge was overestimated (>150%), and water withdrawal was underestimated (<60%)—is considered overly optimistic. Conversely, Sydney's score is considered overly pessimistic, as its river discharge was underestimated (<60%) and its water withdrawal was overestimated (>150%). Nevertheless, with a score of 0.99, Sydney can be described as a city with a low risk of water scarcity.

https://doi.org/10.5194/egusphere-2026-5322
Preprint. Discussion started: 9 September 2026
© Author(s) 2026. CC BY 4.0 License.

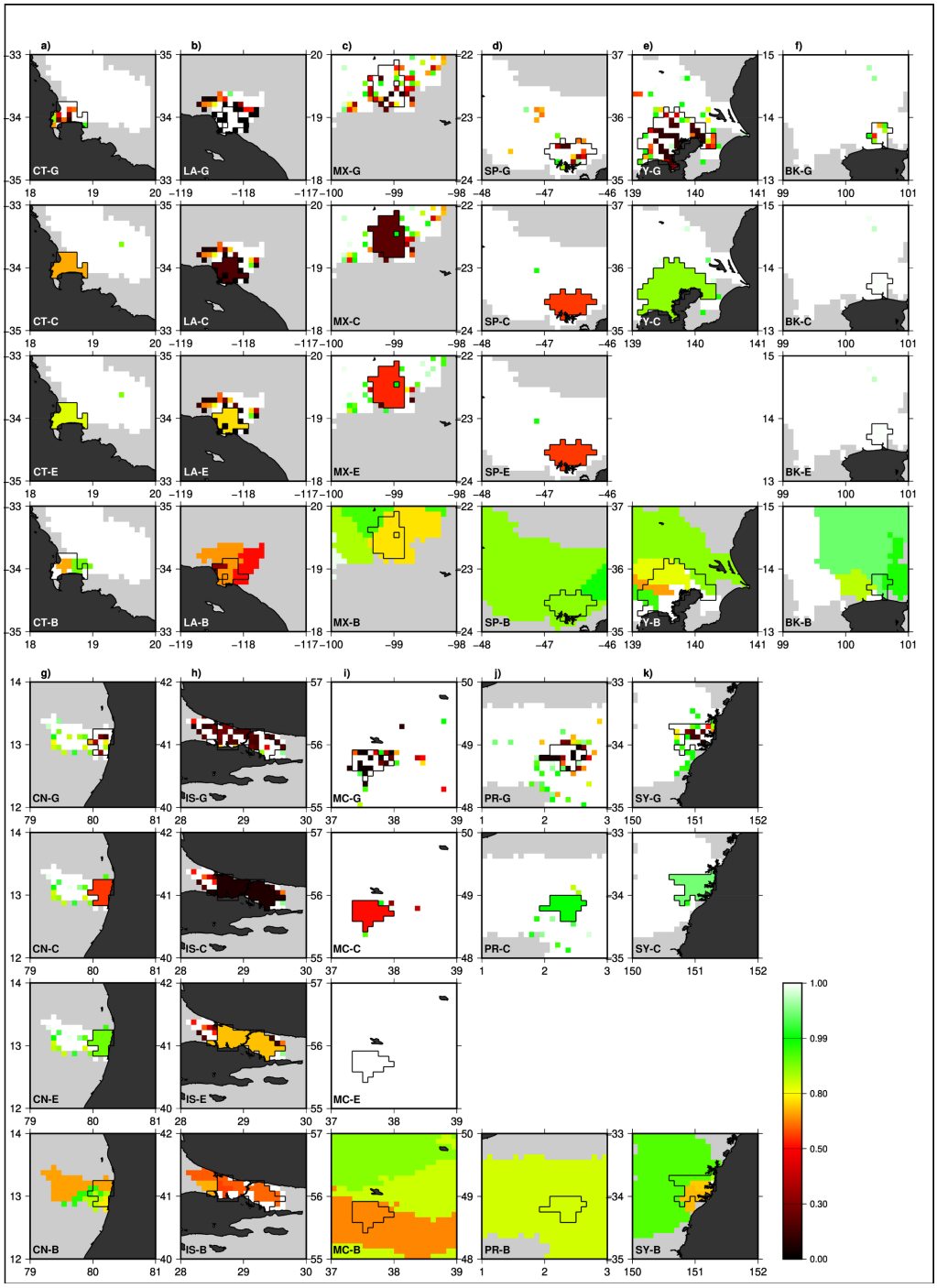

Figure 5. The CAD scores of a) Los Angeles (LA), b) Paris (PR), c) Moscow (MC), d) Mexico City (MX), e) Istanbul (IS), f) Chennai (CN), g) Bangkok (BK), h) Tokyo (TY), i) Sydney (SY), j) São Paulo (SP), and k) Cape Town (CT). The top, upper-middle, lower-middle, and bottom sub-panels show grid-based, city-based without external water sources (the URB run), city-based with external water sources (the EXT run), and basin-based assessment, respectively. Only the city and surrounding area are shown. The results for the EXT runs are not shown for Tokyo, Paris, and Sydney because these cities have no external water sources.

https://doi.org/10.5194/egusphere-2026-5322
Preprint. Discussion started: 9 September 2026
© Author(s) 2026. CC BY 4.0 License.

Table 4. The CAD scores for the URB (enabling the city sub-model without external sources) and EXT (with external water sources). Hanasaki et al. (2018a) argued that CAD scores >0.99, >0.8, and >0.5 are categorized as low, moderate, and high stress, respectively. For grid-level assessment, the range indicates the minimum and maximum CAD scores within the city boundary. The number in brackets shows the average. For basin-level assessment, the scores of the rivers flowing into each city are shown (a single CAD score for cities with a single river flowing into them). The order is the same as in Table 3.

	URB			EXT
City	Grid-level	City-level	Basin-level	City-level
Cape Town	0.09-1.00 (0.80)	0.70	1.00, 0.90, 0.70	0.82
Los Angeles	0.00-1.00 (0.69)	0.18	0.68, 0.51, 0.67	0.76
Mexico City	0.06-1.00 (0.83)	0.21	0.94, 0.77	0.54
São Paulo	0.14-1.00 (0.84)	0.56	0.88	0.56
Tokyo	0.08-1.00 (0.69)	0.88	0.88, 0.82, 0.95, 0.69	--
Bangkok	0.52-1.00 (0.93)	1.00	0.99, 0.97, 0.85	1.00
Chennai	0.14-1.00 (0.80)	0.56	0.69, 0.96, 0.85	0.91
Istanbul	0.16-1.00 (0.64)	0.07	0.62, 0.60, 0.70, 0.60	0.73
Moscow	0.02-1.00 (0.61)	0.51	0.66	1.00
Paris	0.02-1.00 (0.99)	0.99	0.83	--
Sydney	0.08-1.00 (0.82)	0.99	0.93, 0.72, 0.74	--

3.3 External water resources

Under the URB run, CAD exceeds 0.80 (the threshold for moderate water stress in Hanasaki et al. (2018b) for only four cities: Tokyo, Bangkok, Paris, and Sydney (see Table 4). This implies that the remaining cities may receive water from external sources. When external water sources are considered (i.e., under the EXT run), CAD increased drastically. For three cities, CAD exceeds 0.80 (Cape Town, Chennai, and Moscow; Table 4). Although slightly below 0.80, the score also improved drastically in two cities: Los Angeles and Istanbul.

The CAD scores for two cities remained low, namely São Paulo and Mexico City. This is partly attributed to technical issues with the model. For São Paulo, the city water inlet in the HUM database is located in the east of the city (see Fig. 2j). Actually, it correctly locates the main channel of the Tiete River. However, the flow rate is limited relative to the city's vast water requirements, resulting in a relatively low CAD index in URB. As the map clearly shows, the city is located in the uppermost river basin, and the water source is not well represented at the uppermost point of the main channel (i.e., the city also receives water from other tributaries in the basin; see Fig 2j). Mexico City receives water from the Lerma and Cutzamala Rivers in the west. Because the river sequence of H08 at the water source of the Lerma River is greater than both of the two city water inlets, the explicit aqueduct did not work.

The CAD difference between the URB and EXT runs indicates the reliance on external water sources of the studied cities. More than (or nearly) half of the water is supplied from external sources in Los Angeles, Mexico City, Istanbul, and Moscow.

https://doi.org/10.5194/egusphere-2026-5322
Preprint. Discussion started: 9 September 2026
© Author(s) 2026. CC BY 4.0 License.

It brings two key messages. First, it emphasizes the importance of city-specific water scarcity assessment. These kinds of conditions cannot be explored by basin-level water assessment. Second, it underlines the importance of collecting city-specific databases on the location of water sources. Such work has been partly completed by McDonald et al. (2014) and Flörke et al. (2018), but it should be further enhanced and updated.

3.4 Uncertainties and challenges

In this paper, we demonstrated a method for presenting city-level water scarcity assessment using a global hydrological model. Although there are considerable advantages over conventional grid-level and basin-level approaches, some challenges remain. In the following part, we discuss four areas of uncertainty and challenges.

Since water scarcity indices are derived from GHM outputs, the reliability of the assessment depends on the accuracy of these output data, particularly in estimating river discharge and municipal water withdrawals. As seen in Section 3.1, these data well reproduced the historical data in some cities, but not in others. Although river discharge is the most fundamental output variable in hydrological modeling, it remains challenging at the global scale (Heinicke et al., 2024). Continuous efforts on input data improvement (Muñoz-Sabater et al., 2021) and parameter optimization (Tsai et al., 2021) are required. For the latter, the availability of observed river discharge data is the key, but they are limited, particularly in vast areas of Asia, Africa, and other regions (Elmi et al., 2024). The limited accuracy of municipal water withdrawals is also a significant issue. A city-level global inventory of water use should be developed.

In this study, the groundwater fraction to total water requirement is fixed at the regional level. To be precise, since data were available for about one country per UN region, we extrapolated the values from the countries with available data to the entire region (Hanasaki et al., 2018a). Due to this limitation, the assessment of cities having a distinct fraction from the region can be misleading. A database of the groundwater fraction of total water demand for the world's major cities should be urgently developed, along with reliable groundwater models that accurately estimate groundwater availability.

As seen in Section 3.3, large cities do not always rely on rivers flowing in for water resources but rather on external rivers. Although the former is available in the HUM database, the latter is not. As far as the authors know, except for McDonald et al. (2014) and Flörke et al. (2018), such information has not yet been compiled globally. Furthermore, water resources infrastructure, including dams, canals, aqueducts, and desalination plants, plays a crucial role in water supply in regular and emergency situations. Ideally, not only the location of the water source but also the capacity of water transfer or production is needed (e.g., channel or pipe capacity, agreed rate of water transfer, etc.). Some cities disclose a geographical map of water sources, water purification plants, and the water supply area with some key numbers (Bureau of Waterworks Tokyo Metropolitan Government, 2025). Such comprehensive disclosure of water information is encouraged to enhance the accuracy of global city-level water assessment.

As discussed in the Methods Section, the city sub-model does not allow repeated use of water within the urban boundary. This perhaps works for most cities, but exceptions exist. At least in the Tama River in Tokyo, some wastewater treatment plants are

https://doi.org/10.5194/egusphere-2026-5322
Preprint. Discussion started: 9 September 2026
© Author(s) 2026. CC BY 4.0 License.

located upstream of water purification plants within the city boundary. When such multiple uses of water within a city take place, our method may overestimate water scarcity.

Lastly, the limitations of the new city sub-model are revisited. First, the cities located in the uppermost basin need caution (e.g., São Paulo). The city sub-model's algorithm accounts only for the water availability in one inlet grid cell per basin (i.e., the main channel). In the case of São Paulo, only the river discharge of the main stem of the Tietê River, flowing from the southeast, is considered the city's water availability, while the tributaries, including large reservoirs on the left bank, are neglected. Although the city-sub model enables the consistent comparison of the world's cities, it may over- or underestimate water scarcity risks in some cases. Second, water transfer from external water sources is expressed using the function of the explicit aqueduct of the H08 model (Hanasaki et al., 2018a). Although simple and implementable to other GHMs, the restriction that the origin river sequence must be higher than the destination should be well noted.

4 Conclusions

This study proposed a novel method for representing cities in GHMs. We posed two research questions. The first question was: How well can we represent the hydrological process of cities in GHMs? We proposed a novel algorithm to represent cities' water availability and requirements using the newly developed global city boundary dataset, called HUM (Kajiyama et al., 2026). The concept of the city water inlet and outlet successfully aggregates water availability, abstraction, and drainage of cities. The second question was: What is the advantage of city-level water scarcity assessment compared to traditional basin- or grid-level assessments? We applied the global water resources model with the new city algorithm to 11 selected cities worldwide and compared conventional grid- and basin-level water scarcity assessments with the new city-level one. The results clearly show the advantage of the new method, which presents a single water-scarcity score for each city. The conventional approaches display a considerable range of water scarcity scores among grid cells and the rivers flowing into the cities, which is simply uninterpretable. Moreover, the former is based on unrealistic simulations that allow cell-wise cascading water use from upstream to downstream because of ignoring city pipelines, and the latter includes water availability and use in vast non-urban areas in the assessment.

Our new algorithm opens the pathway to the city-level global water scarcity assessment. It leads to fully utilizing high-resolution (i.e., 5 arc minutes and finer) global hydrological simulations that include thousands of large cities, each spanning multiple grid cells. Since the HUM dataset can be updated with the global population density map (Kajiyama et al., 2026), the model is applicable for future projections under various population scenarios.

Cities, particularly large ones, attract people, industry, and capital. A projection by the United Nations indicates that two-thirds of the growth in the world's population between now and 2050 will occur in cities, and the number of megacities (10 million inhabitants or more) continues to grow (United Nations, 2025). Meeting growing urban water requirements under a changing climate will be an increasingly important and challenging task in this century. City-level global water resources modeling and assessment will be useful for understanding the issue and identifying essential solutions.

https://doi.org/10.5194/egusphere-2026-5322
Preprint. Discussion started: 9 September 2026
© Author(s) 2026. CC BY 4.0 License.

Appendix A Elevation correction and rainfall-snowfall separation

Throughout this appendix, the subscripts f and c denote a value defined on the fine 5-arc-minute grid cells and on the coarse 30-arc-minute grid cells, respectively. Near-surface air temperature T was then corrected with the environmental lapse rate of Γ, 6.5×10^{-3} K m^{-1}:

$$T_f = T_c - \Gamma \Delta z \quad \text{(A-1)}$$

where $\Delta z = z_f - z_c$ is the elevation difference between the fine cell and the coarse cell. Surface pressure P was adjusted for the elevation difference as

$$P_f = P_c \exp\left(-\frac{g\Delta z}{R_d \bar{T}}\right) \quad \text{(A-2)}$$

where $g = 9.81$ m s^{-2} is the gravitational acceleration, $R_d = 287.06$ J kg^{-1} K^{-1} is the gas constant for dry air, and is the layer-mean temperature. The specific humidity q_f was computed as follows. Using bilinearly interpolated relative humidity RH_f, the saturation water-vapor pressure e_s and the partial water-vapor pressure e_s were calculated at T_f following Bolton (1980):

$$e_s(T_f) = 611.2 \exp\left[\frac{17.67(T_f - 273.15)}{(T_f - 273.15) + 243.5}\right] \quad \text{(A-3)}$$

$$e_f = \frac{RH_f}{100} \cdot e_s(T_f) \quad \text{(A-4)}$$

$$q_f = \frac{0.622 \cdot e_f}{P_f - 0.378 \cdot e_f} \quad \text{(A-5)}$$

Downwelling longwave radiation LW_f was scaled following the NLDAS convention (Cosgrove et al., 2003).

$$LW_f = LW_c \left(\frac{T_f}{T_c}\right)^4 \quad \text{(A-6)}$$

Daily precipitation was partitioned into rainfall and snowfall at the 5-arc-minute resolution following the scheme of Yamazaki (2001) using the critical air temperature T^*:

$$T^* = 284.16 - 1.5 \cdot e_f \quad \text{(A-7)}$$

The total daily precipitation was assigned entirely to rainfall when $T_f > T^*$ and entirely to snowfall otherwise. Figure A-1 shows a comparison of the daily meteorological forcing in South Asia.

https://doi.org/10.5194/egusphere-2026-5322
Preprint. Discussion started: 9 September 2026
© Author(s) 2026. CC BY 4.0 License.

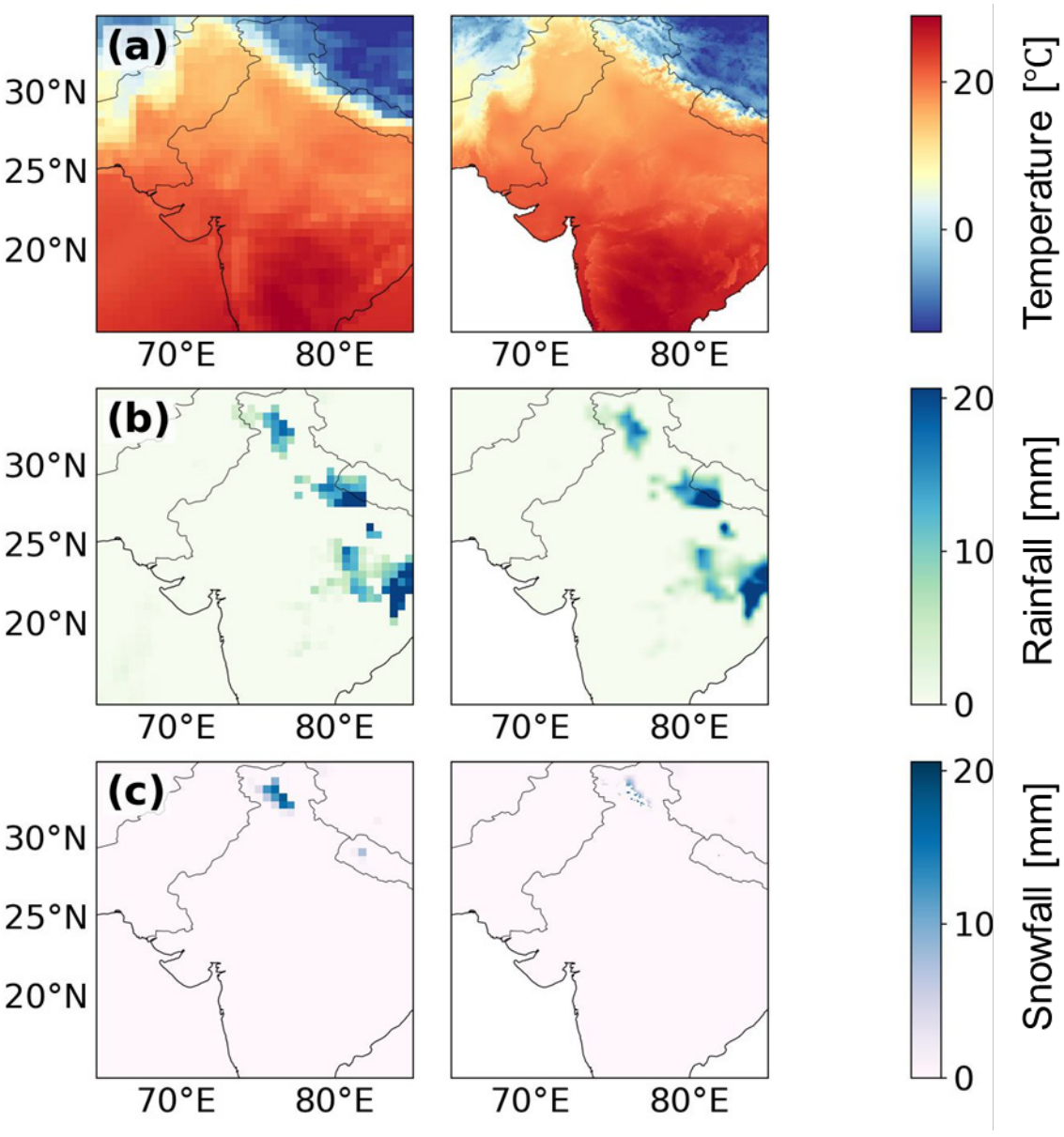

435 **Figure A1. Comparison of the daily meteorological forcing in South Asia on 15 February 2019, before (left, 30 arc-minute W5E5) and after (right, 5 arc-minute downscaled) the elevation. (a) near-surface air temperature, (b) daily rainfall, and (c) daily snowfall.**

https://doi.org/10.5194/egusphere-2026-5322
Preprint. Discussion started: 9 September 2026
© Author(s) 2026. CC BY 4.0 License.

Code and data availability

The code is available at https://doi.org/10.5281/zenodo.22218765 (Hanasaki, 2026). The input meteorological data is available at A-PLAT Pro (https://ccca-scenario.nies.go.jp/index_en.html). The input geographical data is available at H08 Home (https://h08.nies.go.jp/).

Author contributions

NH and SK designed the experiments, and NH, KK, and YT carried them out. NH developed the model code and performed the simulations. KK, YT, KY, and YM curated the data. NH prepared the manuscript with contributions from all co-authors.

Competing interests

The authors declare no competing interests.

Disclaimer

Copernicus Publications remains neutral with regard to jurisdictional claims made in the text, published maps, institutional affiliations, or any other geographical representation in this paper. While Copernicus Publications makes every effort to include appropriate place names, the final responsibility lies with the authors. Views expressed in the text are those of the authors and do not necessarily reflect the views of the publisher.

Acknowledgements

The authors acknowledge Keisuke Doi, Aoba Kato, and Kazuhide Kakiuchi for their contributions to the earlier stage of model development. The authors gratefully acknowledge the Global Runoff Data Centre (GRDC) in 56068 Koblenz, Germany for providing the discharge data used in this study. We used Grammarly to proofread our English text.

Financial support

This study was supported by the Environment Research and Technology Development Fund of the ERCA (JPMEERF23S21120) funded by the Ministry of the Environment. NH is supported by JSPS KAKENHI Grant Number 26H02161.

https://doi.org/10.5194/egusphere-2026-5322
Preprint. Discussion started: 9 September 2026
© Author(s) 2026. CC BY 4.0 License.

Review statement

The review statement will be added by Copernicus Publications listing the handling editor as well as all contributing referees according to their status anonymous or identified.

References

Ai, Z., Ishihama, F., and Hanasaki, N.: Mapping Current and Future Seawater Desalination Plants Globally Using Species Distribution Models, Water Resources Research, 58, e2021WR031156, https://doi.org/10.1029/2021WR031156, 2022.

Alcamo, J., Döll, P., Henrichs, T., Kaspar, F., Lehner, B., Rösch, T., and Siebert, S.: Global estimates of water withdrawals and availability under current and future "business-as-usual" conditions, Hydrological Sciences Journal-Journal Des Sciences Hydrologiques, 48, 339-348, https://doi.org/10.1623/hysj.48.3.339.45278, 2003.

Bolton, D.: The Computation of Equivalent Potential Temperature, Monthly Weather Review, 108, 1046-1053, https://doi.org/10.1175/1520-0493(1980)108<1046:TCOEPT>2.0.CO;2, 1980.

Tokyo's Water Sources and Water Supply Areas by Water Treatment Plant: https://www.waterworks.metro.tokyo.lg.jp/suigen/map, access: June 10, 2026, 2025.

Burek, P., Satoh, Y., Kahil, T., Tang, T., Greve, P., Smilovic, M., Guillaumot, L., Zhao, F., and Wada, Y.: Development of the Community Water Model (CWatM v1.04) – a high-resolution hydrological model for global and regional assessment of integrated water resources management, Geosci. Model Dev., 13, 3267-3298, 10.5194/gmd-13-3267-2020, 2020.

Center for International Earth Science Information Network-CIESIN-Columbia University: Gridded Population of the World, Version 4 (GPWv4): Population Density, Revision 11 (Version 4.11) NASA Socioeconomic Data and Applications Center, Palisades, NY, https://doi.org/10.7927/H7949C7926VHW, 2017.

Cosgrove, B. A., Lohmann, D., Mitchell, K. E., Houser, P. R., Wood, E. F., Schaake, J. C., Robock, A., Marshall, C., Sheffield, J., Duan, Q., Luo, L., Higgins, R. W., Pinker, R. T., Tarpley, J. D., and Meng, J.: Real-time and retrospective forcing in the North American Land Data Assimilation System (NLDAS) project, Journal of Geophysical Research: Atmospheres, 108, https://doi.org/10.1029/2002JD003118, 2003.

Cucchi, M., Weedon, G. P., Amici, A., Bellouin, N., Lange, S., Müller Schmied, H., Hersbach, H., and Buontempo, C.: WFDE5: bias-adjusted ERA5 reanalysis data for impact studies, Earth Syst. Sci. Data, 12, 2097-2120, 10.5194/essd-12-2097-2020, 2020.

Di Vittorio, C. A., and Georgakakos, A. P.: Hydrologic Modeling of the Sudd Wetland using Satellite-based Data, Journal of Hydrology: Regional Studies, 37, 100922, https://doi.org/10.1016/j.ejrh.2021.100922, 2021.

Döll, P., and Lehner, B.: Validation of a new global 30-min drainage direction map, Journal of Hydrology, 258, 214-231, 2002.

Elmi, O., Tourian, M. J., Saemian, P., and Sneeuw, N.: Remote Sensing-Based Extension of GRDC Discharge Time Series - A Monthly Product with Uncertainty Estimates, Scientific Data, 11, 240, 10.1038/s41597-024-03078-6, 2024.

Flörke, M., Schneider, C., and McDonald, R. I.: Water competition between cities and agriculture driven by climate change and urban growth, Nature Sustainability, 1, 51-58, 10.1038/s41893-017-0006-8, 2018.

GreenCape: Water: Market Intelligence Report 2019, GreenCape, Cape Town, South Africa, 58, 2019.

Haddeland, I., Clark, D. B., Franssen, W., Ludwig, F., Voß, F., Arnell, N. W., Bertrand, N., Best, M., Folwell, S., Gerten, D., Gomes, S., Gosling, S. N., Hagemann, S., Hanasaki, N., Harding, R., Heinke, J., Kabat, P., Koirala, S., Oki, T., Polcher, J., Stacke, T., Viterbo, P., Weedon, G. P., and Yeh, P.: Multimodel Estimate of the Global Terrestrial Water Balance: Setup and First Results, Journal of Hydrometeorology, 12, 869-884, 10.1175/2011jhm1324.1, 2011.

Hanasaki, N., Kanae, S., and Oki, T.: A reservoir operation scheme for global river routing models, Journal of Hydrology, 327, 22-41, 10.1016/j.jhydrol.2005.11.011, 2006.

Hanasaki, N., Kanae, S., Oki, T., Masuda, K., Motoya, K., Shirakawa, N., Shen, Y., and Tanaka, K.: An integrated model for the assessment of global water resources - Part 1: Model description and input meteorological forcing, Hydrol. Earth Syst. Sci., 12, 1007-1025, 10.5194/hess-12-1007-2008, 2008a.

© Author(s) 2026. CC BY 4.0 License.

Hanasaki, N., Kanae, S., Oki, T., Masuda, K., Motoya, K., Shirakawa, N., Shen, Y., and Tanaka, K.: An integrated model for the assessment of global water resources - Part 2: Applications and assessments, Hydrol. Earth Syst. Sci., 12, 1027-1037, 10.5194/hess-12-1027-2008, 2008b.

Hanasaki, N., Yoshikawa, S., Kakinuma, K., and Kanae, S.: A seawater desalination scheme for global hydrological models, Hydrology and Earth System Sciences, 20, 4143-4157, 10.5194/hess-20-4143-2016, 2016.

Hanasaki, N., Yoshikawa, S., Pokhrel, Y., and Kanae, S.: A global hydrological simulation to specify the sources of water used by humans, Hydrology and Earth System Sciences, 22, 789-817, 10.5194/hess-22-789-2018, 2018a.

Hanasaki, N., Yoshikawa, S., Pokhrel, Y., and Kanae, S.: A Quantitative Investigation of the Thresholds for Two Conventional Water Scarcity Indicators Using a State-of-the-Art Global Hydrological Model With Human Activities, Water Resources Research, 54, 8279-8294, 10.1029/2018WR022931, 2018b.

Hanasaki, N.: H08 (city.v1) [Computer software], Zenodo, https://doi.org/10.5281/zenodo.22218766, 2026.

He, C., Liu, Z., Wu, J., Pan, X., Fang, Z., Li, J., and Bryan, B. A.: Future global urban water scarcity and potential solutions, Nature Communications, 12, 4667, 10.1038/s41467-021-25026-3, 2021.

Heinicke, S., Volkholz, J., Schewe, J., Gosling, S. N., Müller Schmied, H., Zimmermann, S., Mengel, M., Sauer, I. J., Burek, P., Chang, J., Kou-Giesbrecht, S., Grillakis, M., Guillaumot, L., Hanasaki, N., Koutroulis, A. G., Otta, K., Qi, W., Satoh, Y., Stacke, T., Yokohata, T., and Frieler, K.: Global hydrological models continue to overestimate river discharge, Environmental Research Letters, 19, 074005, 10.1088/1748-9326/ad52b0, 2024.

Interfax-Russia: Water consumption in Moscow fell by a quarter on January 1, Interfax-Russia, https://www.interfax-russia.ru/moscow/news/potreblenie-vody-v-moskve-upalo-na-chetvert-1-yanvarya, 2022.

Kajiyama, K., Hanasaki, N., and Kanae, S.: City boundaries for global urban water scarcity assessment, Scientific Data, 13, 657, 10.1038/s41597-026-06933-w, 2026.

Klein Goldewijk, K., Beusen, A., Doelman, J., and Stehfest, E.: Anthropogenic land use estimates for the Holocene – HYDE 3.2, Earth Syst. Sci. Data, 9, 927-953, 10.5194/essd-9-927-2017, 2017.

Knoben, W. J. M., Freer, J. E., and Woods, R. A.: Technical note: Inherent benchmark or not? Comparing Nash–Sutcliffe and Kling–Gupta efficiency scores, Hydrol. Earth Syst. Sci., 23, 4323-4331, 10.5194/hess-23-4323-2019, 2019.

Kummu, M., Ward, P. J., de Moel, H., and Varis, O.: Is physical water scarcity a new phenomenon? Global assessment of water shortage over the last two millennia, Environmental Research Letters, 5, 034006, 10.1088/1748-9326/5/3/034006, 2010.

Lange, S., Menz, C., Gleixner, S., Cucchi, M., Weedon, G. P., Amici, A., Bellouin, N., Schmied, H. M., Hersbach, H., Buontempo, C., and Cagnazzo, C.: WFDE5 over land merged with ERA5 over the ocean (W5E5 v2.0), ISIMIP Repository, https://doi.org/10.48364/ISIMIP.342217 2021.

LaVanchy, G. T., Kerwin, M. W., and Adamson, J. K.: Beyond 'Day Zero': insights and lessons from Cape Town (South Africa), Hydrogeology Journal, 27, 1537-1540, 10.1007/s10040-019-01979-0, 2019.

Lehner, B., Liermann, C. R., Revenga, C., Vörösmarty, C., Fekete, B., Crouzet, P., Döll, P., Endejan, M., Frenken, K., Magome, J., Nilsson, C., Robertson, J. C., Rödel, R., Sindorf, N., and Wisser, D.: High-resolution mapping of the world's reservoirs and dams for sustainable river-flow management, Front. Ecol. Environ., 9, 494-502, 10.1890/100125, 2011.

Los Angeles Department of Water and Power (LADWP): 2022-23 Briefing Book, LADWP, Los Angeles, CA, 63, 2023.

McDonald, R. I., Weber, K., Padowski, J., Flörke, M., Schneider, C., Green, P. A., Gleeson, T., Eckman, S., Lehner, B., Balk, D., Boucher, T., Grill, G., and Montgomery, M.: Water on an urban planet: Urbanization and the reach of urban water infrastructure, Global Environmental Change, 27, 96-105, https://doi.org/10.1016/j.gloenvcha.2014.04.022, 2014.

Medina-Rivas, C. M., Rodríguez-Tapia, L., Morales-Novelo, J. A., and Revollo-Fernández, D. A.: Spatial inequality of domestic water consumption in Mexico city, Water Resources and Economics, 40, 100210, https://doi.org/10.1016/j.wre.2022.100210, 2022.

Metropolitan Waterworks Authority: Quality Water for Quality Living, Metropolitan Waterworks Authority, Bangkok, Thailand, 184, 2024.

Müller Schmied, H., Trautmann, T., Ackermann, S., Cáceres, D., Flörke, M., Gerdener, H., Kynast, E., Peiris, T. A., Schiebener, L., Schumacher, M., and Döll, P.: The global water resources and use model WaterGAP v2.2e: description and evaluation of modifications and new features, Geosci. Model Dev., 17, 8817-8852, 10.5194/gmd-17-8817-2024, 2024.

Muñoz-Sabater, J., Dutra, E., Agustí-Panareda, A., Albergel, C., Arduini, G., Balsamo, G., Boussetta, S., Choulga, M., Harrigan, S., Hersbach, H., Martens, B., Miralles, D. G., Piles, M., Rodríguez-Fernández, N. J., Zsoter, E., Buontempo, C.,

https://doi.org/10.5194/egusphere-2026-5322
Preprint. Discussion started: 9 September 2026
© Author(s) 2026. CC BY 4.0 License.

and Thépaut, J. N.: ERA5-Land: a state-of-the-art global reanalysis dataset for land applications, Earth Syst. Sci. Data, 13, 4349-4383, 10.5194/essd-13-4349-2021, 2021.
OECD: Adapting the Paris Metropolitan Area to a Water-Scarce Future, OECD Publishing, Paris, France, 206, 2025.
Schewe, J., Heinke, J., Gerten, D., Haddeland, I., Arnell, N. W., Clark, D. B., Dankers, R., Eisner, S., Fekete, B. M., Colón-González, F. J., Gosling, S. N., Kim, H., Liu, X., Masaki, Y., Portmann, F. T., Satoh, Y., Stacke, T., Tang, Q., Wada, Y., Wisser, D., Albrecht, T., Frieler, K., Piontek, F., Warszawski, L., and Kabat, P.: Multimodel assessment of water scarcity under climate change, Proceedings of the National Academy of Sciences, 111, 3245-3250, 10.1073/pnas.1222460110, 2014.
Secretaria Nacional de Saneamento (SNS) Ministério do Desenvolvimento Regional (MDR): 25º Diagnóstico dos Serviços de Água e Esgotos – 2019, SNS/MDR, Brasília, Brasil, Sistema Nacional de Informações sobre Saneamento, 183, 2020.
Su, J., Miao, C., Zwiers, F., Beck, H., Jones, P., Sun, Q., Slater, L. J., Berghuijs, W. R., Wada, Y., Rosenfeld, D., Gou, J., Wu, Y., Tarolli, P., Borrelli, P., Panagos, P., Alexander, L. V., Zhang, Q., Hu, J., Min, S.-K., Samaniego, L., Duan, Q., Destouni, G., Marengo, J. A., Modarres, R., and Sorooshian, S.: Precipitation observing network gaps limit climate change impact assessment, Nature, 652, 119-125, 10.1038/s41586-026-10300-5, 2026.
Sutanudjaja, E. H., van Beek, R., Wanders, N., Wada, Y., Bosmans, J. H. C., Drost, N., van der Ent, R. J., de Graaf, I. E. M., Hoch, J. M., de Jong, K., Karssenberg, D., López López, P., Peßenteiner, S., Schmitz, O., Straatsma, M. W., Vannametee, E., Wisser, D., and Bierkens, M. F. P.: PCR-GLOBWB 2: a 5 arcmin global hydrological and water resources model, Geosci. Model Dev., 11, 2429-2453, 10.5194/gmd-11-2429-2018, 2018.
Sydney Water: Water Conservation 2023–24: Performance and Forward Plan, Sydney Water, Sydney, Australia, 2024.
The Energy and Resources Institute (TERI): Water Sustainability Assessment of Chennai Metropolitan Area, TERI, New Delhi, India, 77, 2021.
Tsai, W.-P., Feng, D., Pan, M., Beck, H., Lawson, K., Yang, Y., Liu, J., and Shen, C.: From calibration to parameter learning: Harnessing the scaling effects of big data in geoscientific modeling, Nature Communications, 12, 5988, 10.1038/s41467-021-26107-z, 2021.
Turkish Statistical Institute: Water and Wastewater Statistics, 2022, Turkish Statistical Institute, https://veriportali.tuik.gov.tr/en/press/49607, 2023.
United Nations: World Urbanization Prospects: The 2018 Revision, United Nations, New York, USA, 103, 2019.
United Nations: World Urbanization Prospects 2025: Summary of Results, UN DESA/POP/2025/TR/, New York, United Nations, 2025.
Vanham, D., Alfieri, L., Flörke, M., Grimaldi, S., Lorini, V., de Roo, A., and Feyen, L.: The number of people exposed to water stress in relation to how much water is reserved for the environment: a global modelling study, The Lancet Planetary Health, 5, e766-e774, 10.1016/S2542-5196(21)00234-5, 2021.
Vörösmarty, C. J., Green, P., Salisbury, J., and Lammers, R. B.: Global water resources: Vulnerability from climate change and population growth, Science, 289, 284-288, 10.1126/science.289.5477.284, 2000.
Wada, Y., de Graaf, I. E. M., and van Beek, L. P. H.: High-resolution modeling of human and climate impacts on global water resources, Journal of Advances in Modeling Earth Systems, 8, 735-763, 10.1002/2015MS000618, 2016.
Water Resources Department Water Management and Land Conservation Bureau Ministry of Land Infrastructure Transport and Tourism (MLIT): Current Status of Japan's Water Resources 2025 Edition, Water Resources Department, Water Management and Land Conservation Bureau, MLIT, Tokyo, Japan, 232, 2025.
Wheater, H.: Why is arid zone hydrology a scientific desert - and how does the hydrological community move forward?, Environmental Modelling & Software, 192, 106561, https://doi.org/10.1016/j.envsoft.2025.106561, 2025.
Yamazaki, D., Ikeshima, D., Tawatari, R., Yamaguchi, T., O'Loughlin, F., Neal, J. C., Sampson, C. C., Kanae, S., and Bates, P. D.: A high-accuracy map of global terrain elevations, Geophys. Res. Lett., 44, 5844-5853, https://doi.org/10.1002/2017GL072874, 2017.
Yamazaki, D., Ikeshima, D., Sosa, J., Bates, P. D., Allen, G. H., and Pavelsky, T. M.: MERIT Hydro: A High-Resolution Global Hydrography Map Based on Latest Topography Dataset, Water Resources Research, 55, 5053-5073, https://doi.org/10.1029/2019WR024873, 2019.
Yamazaki, T.: A one-dimensional land surface model adaptable to intensely cold regions and its application in Eastern Siberia, Journal of the Meteorological Society of Japan, 79, 1107-1118, https://doi.org/10.2151/jmsj.79.1107, 2001.

https://doi.org/10.5194/egusphere-2026-5322
Preprint. Discussion started: 9 September 2026
© Author(s) 2026. CC BY 4.0 License.

Yoshida, T., Hanasaki, N., Nishina, K., Boulange, J., Okada, M., and Troch, P. A.: Inference of Parameters for a Global Hydrological Model: Identifiability and Predictive Uncertainties of Climate-Based Parameters, Water Resources Research, 58, e2021WR030660, https://doi.org/10.1029/2021WR030660, 2022.

Zaherpour, J., Gosling, S. N., Mount, N., Schmied, H. M., Veldkamp, T. I. E., Dankers, R., Eisner, S., Gerten, D., Gudmundsson, L., Haddeland, I., Hanasaki, N., Kim, H., Leng, G., Liu, J., Masaki, Y., Oki, T., Pokhrel, Y., Satoh, Y., Schewe, J., and Wada, Y.: Worldwide evaluation of mean and extreme runoff from six global-scale hydrological models that account for human impacts, Environmental Research Letters, 13, 10.1088/1748-9326/aac547, 2018.